



Bunzel, A., Kries, H., Marchetti, L., Zeymer, C., Mittl, P. R. E., Mulholland, A., & Hilvert, D. (2019). Emergence of a Negative Activation Heat Capacity during Evolution of a Designed Enzyme. *Journal of the American Chemical Society*, 141(30), 11745-11748. <https://doi.org/10.1021/jacs.9b02731>

Peer reviewed version

Link to published version (if available):
[10.1021/jacs.9b02731](https://doi.org/10.1021/jacs.9b02731)

[Link to publication record in Explore Bristol Research](#)
PDF-document

This is the author accepted manuscript (AAM). The final published version (version of record) is available online via ACS Publications at <https://pubs.acs.org/doi/10.1021/jacs.9b02731>. Please refer to any applicable terms of use of the publisher.

University of Bristol - Explore Bristol Research

General rights

This document is made available in accordance with publisher policies. Please cite only the published version using the reference above. Full terms of use are available: <http://www.bristol.ac.uk/red/research-policy/pure/user-guides/ebr-terms/>

Emergence of a negative activation heat capacity during evolution of a designed enzyme

H. Adrian Bunzel[†], Hajo Kries[†], Luca Marchetti[†], Cathleen Zeymer[†], Peer R. E. Mittl[‡], Adrian J. Mulholland[§], Donald Hilvert^{†*}

[†] Laboratory of Organic Chemistry, ETH Zurich, 8093 Zurich, Switzerland

[‡] Department of Biochemistry, University of Zurich, 8057 Zurich, Switzerland

[§] Centre for Computational Chemistry, School of Chemistry, University of Bristol, Bristol BS8 1TS, United Kingdom

Supporting Information Placeholder

ABSTRACT: Temperature influences the reaction kinetics and evolvability of all enzymes. To understand how evolution shapes the thermodynamic drivers of catalysis, we optimized the modest activity of a computationally designed enzyme for an elementary proton transfer reaction by nearly four orders of magnitude over nine rounds of mutagenesis and screening. As theorized for primordial enzymes, the catalytic effects of the original design were almost entirely enthalpic in origin, as were the rate enhancements achieved by laboratory evolution. However, the large reductions in ΔH^\ddagger were partially offset by a decrease in TAS^\ddagger and, unexpectedly, accompanied by a negative activation heat capacity, signaling strong adaptation to the operating temperature. These findings echo reports of temperature-dependent activation parameters for highly evolved natural enzymes, and are relevant to explanations of enzymatic catalysis and adaptation to changing thermal environments.

Wolfenden has shown that the rate accelerations achieved by many natural enzymes have largely enthalpic origins.^{1, 2} If life originated in a hot environment,³⁻⁶ primordial enzymes that shared this trait would have had an evolutionary advantage in sustaining significant rates as the early earth cooled because of their shallow temperature dependence. Thermal adaptation of enzymes has been studied by analysis of modern enzyme homologs,⁷ ancestral sequence reconstruction,⁸ and computation.⁹ Here, instead, we exploited directed evolution at ambient temperature to assess how the thermodynamic drivers of catalysis respond to selection for enhanced activity of an elementary chemical reaction.

Computationally designed enzymes^{10,11} are valuable models of evolutionarily naïve catalysts. They display the modest activities expected for primordial enzymes but can be substantially improved by laboratory evolution.^{12,13} As our starting point, we chose the computational design 1A53-2,¹⁴ which catalyzes the base-promoted E2 elimination of 5-nitrobenzisoxazole (Figure 1). This reaction, the Kemp elimination, is a well-studied model for proton transfer from carbon.^{15,16} 1A53-2 was created by equipping a thermostable indole-3-glycerolphosphate synthetase with a carboxylate base (Glu178), sandwiched between two tryptophan residues, in a pocket tailored for transition state binding.¹⁴ The resulting

catalyst accelerated the Kemp elimination of 5-nitrobenzisoxazole by 7.8×10^4 fold over the uncatalyzed reaction ($k_{\text{cat}}/k_{\text{uncat}}$).

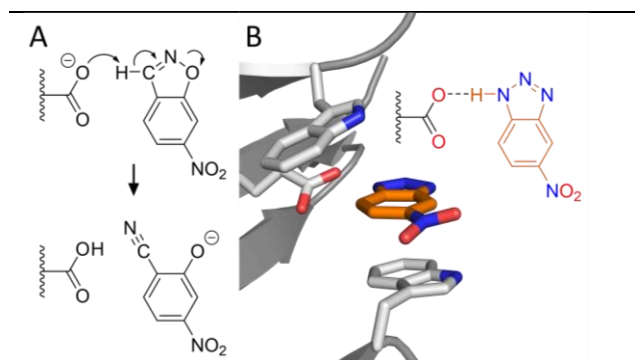


Figure 1. The Kemp elimination catalyzed by 1A53-2. (A) 6-Nitrobenzisoxazole deprotonation affords a salicylonitrile. (B) Glu178 serves as the base in 1A53-2 and forms a hydrogen bond with the inhibitor 5-nitrobenzotriazole (orange carbons).¹⁴

Although 1A53-2 was designed to cleave 5-nitrobenzisoxazole, the crystal structure of the enzyme complexed with 5-nitrobenzotriazole indicated that the less reactive 6-nitrobenzisoxazole would also be a substrate, which we confirmed experimentally ($k_{\text{cat}} = 0.0058 \pm 0.0008 \text{ s}^{-1}$ and $k_{\text{cat}}/K_M = 3.9 \pm 1.4 \text{ M}^{-1} \text{ s}^{-1}$; Table S1). The 1.1×10^4 -fold rate acceleration for this substrate is only 7-times lower than that for 5-nitrobenzisoxazole, mirroring its intrinsic reactivity.¹⁵ The pH-rate profile for the enzyme-catalyzed reaction is bell shaped, with maximum activity achieved at pH 9 (Figure 2C). The apparent ionization constant for the acidic limb suggests that Glu178 has a pK_a of 8.7 ± 0.3 . This value is substantially elevated compared to acetate in aqueous solution or the carboxylic bases in other Kemp eliminases,^{13,17-19} but in accord with the PROPKA prediction of 9.3,²⁰ reflecting the hydrophobic nature of the 1A53-2 active site.

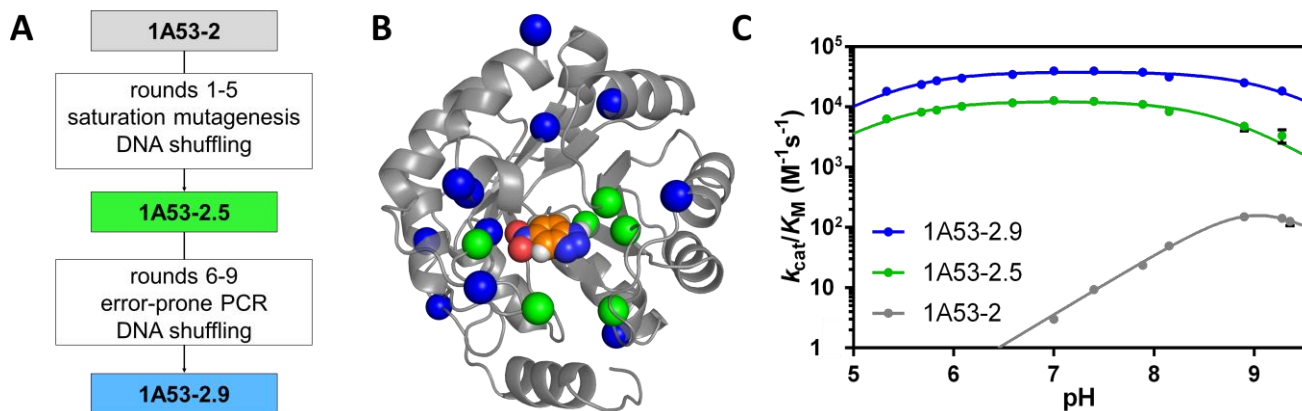


Figure 2. Laboratory evolution of 1A53-2. (A) Evolution was performed in two stages, focusing first on active site residues and then on the entire sequence. (B) Mutations introduced in the first (green spheres) and second (blue spheres) stages are mapped onto the structure of 1A53-2 in complex with 5-nitrobenzotriazole (orange carbons).¹⁴ (C) pH-rate profiles for the starting catalyst (gray), intermediate 1A53-2.5 (green), and evolved 1A53-2.9 enzyme (blue).

To optimize catalytic efficiency, we subjected 1A53-2 to nine rounds of laboratory evolution by screening for 6-nitrobenzisoxazole cleavage at ambient temperature in microtiter plates (Figures 2A, S2, and S3). In the first five rounds, residues lining the active site were targeted by saturation mutagenesis. All first-shell residues were individually randomized with NNK codons and favorable mutations combined by DNA shuffling. In the last four rounds, the entire gene was randomized by error-prone PCR and DNA shuffling. Strikingly, most of the 8,400-fold improvement was achieved during active site optimization, whereas the last four rounds increased efficiency only threefold.

The most active variant, 1A53-2.9, cleaves 6-nitrobenzisoxazole with a 120-fold preference over 5-nitrobenzisoxazole. Like the evolutionary intermediate 1A53-2.5, 1A53-2.9 is active over a much broader pH range than the starting design due to a large decrease in the apparent pK_a of the catalytic base to 5.4 ± 0.1 (Figure 2C). At pH 7.0 and 25 °C, k_{cat} and k_{cat}/K_M were $24 \pm 2 \text{ s}^{-1}$ and $40,900 \pm 5,800 \text{ M}^{-1} \text{ s}^{-1}$, respectively (Table S1). The resulting 4.2×10^7 -fold rate acceleration exceeds that of many other engineered enzymes¹⁷⁻¹⁹ and catalytic antibodies^{21, 22} and is only 15-times below that of HG3.17,¹³ the most active Kemp eliminase known (Table S3). Comparison of k_{cat}/K_M with the second-order rate constant for the acetate-promoted reaction (k_{AcO^-}) further shows that Glu178 is a $>5 \times 10^9$ -fold better base than a simple carboxylate in aqueous solution.

Although 1A53-2.9 failed to crystallize, we solved the x-ray structure of 1A53-2.5 in complex with 5-nitrobenzotriazole at 2.6 Å resolution (PDB ID: 6NW4). The evolved enzyme and the original design have very similar folds ($C\alpha$ rmsd of 0.53 Å) with only a few solvent exposed loops displaying slightly different conformations (Figure S5). The ligand adopts a similar pose in both structures but is better packed by the evolved active site (Figure 3). Mutations such as A157Y, A180C and L184F fill space surrounding the ligand and improve shape complementarity. Tyr157 additionally positions and stabilizes the Glu178 carboxylate through a hydrogen bond, accounting for the decrease in apparent pK_a . Consistent with this interpretation, replacement of Tyr157 with either alanine or

phenylalanine shifts the Glu178 pK_a back to >8 (Figure S4B). The 1A53-2 variants, like most eliminases,^{13,17-19} lack a hydrogen-bonding residue in the vicinity of the phenolic leaving group, so negative charge in the transition state is presumably stabilized by bulk water.

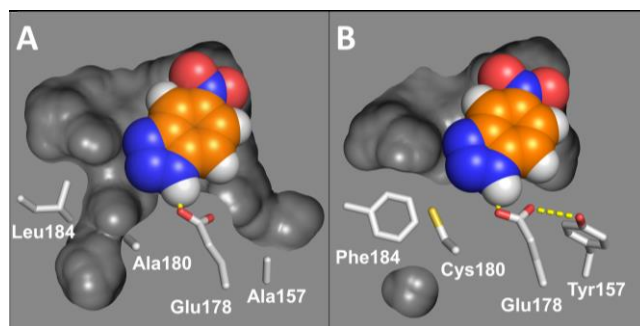


Figure 3. Cut-away view of the (A) 1A53-2 and (B) 1A53-2.5 active sites in complex with 5-nitrobenzotriazole (orange carbons). H-bonding interactions (yellow) and important protein residues (white) are shown.

To assess the thermodynamic origins of the catalytic rate enhancements, we measured the temperature dependence of 6-nitrobenzisoxazole decomposition. The analyses were performed in the k_{cat}/K_M regime due to limited substrate solubility (Figure S6). Nevertheless, the observed trends provide direct insight into the effects of temperature on active site chemistry as opposed to substrate binding, given that k_{cat} increased by almost four orders of magnitude over the course of evolution, whereas K_M decreased only twofold. Focusing on k_{cat}/K_M also enables direct comparison with temperature effects on k_{AcO^-} .

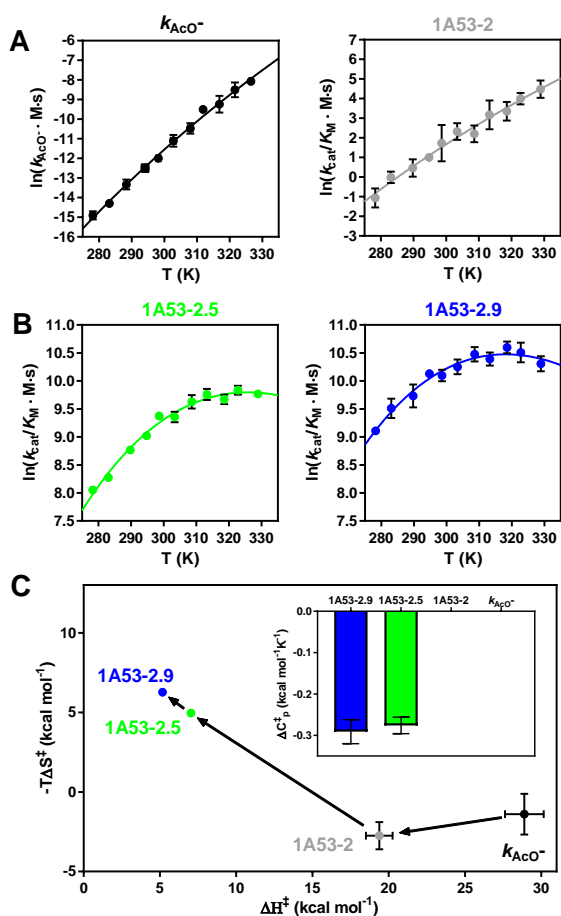


Figure 4. Temperature dependence of the Kemp elimination reaction. (A) The acetate (black) and 1A53-2 (gray) data were fitted to the standard Eyring equation.²³ (B) 1A53-2.5 (green) and 1A53-2.9 (blue) show clear temperature optima and were fitted instead to equation 1 ($T_0 = 298$ K).⁷ (C) At T_0 , substantial decreases in ΔH^\ddagger , partially offset by an unfavorable $-T\Delta S^\ddagger$ term, account for the observed rate enhancements. The error bars denote the standard deviation.

Fitting the data for 1A53-2 to the Eyring equation²³ gave an activation enthalpy (ΔH^\ddagger) of 19.4 ± 0.9 kcal mol $^{-1}$ and an activation entropy (ΔS^\ddagger) of 9.2 ± 2.9 cal mol $^{-1}$ K $^{-1}$ (Figures 4A and S7). The corresponding values for the acetate reaction were $\Delta H^\ddagger = 25.9 \pm 1.3$ kcal mol $^{-1}$ and $\Delta S^\ddagger = 4.7 \pm 4.3$ cal mol $^{-1}$ K $^{-1}$. Thus, in accord with Wolfenden’s predictions for a primitive catalyst, the starting design enhances the rate of the Kemp elimination primarily by lowering ΔH^\ddagger . Moreover, as 1A53-2 was optimized, its temperature dependence became even shallower, indicating a further decrease in ΔH^\ddagger . In contrast to the linear Eyring plots for the reactions promoted by acetate and 1A53-2, the plots for the evolved catalysts show pronounced curvature (Figures 4B and S7) with temperature optima ≥ 18 K above the temperature at which the evolutionary experiments were performed.

Such curvature would occur trivially if the proteins denatured around T_{opt} . This possibility can be excluded in the

case of the evolved eliminases. Structural differences between 1A53-2.5, which shows curvature, and 1A53-2, which does not, are localized at the active site and increased the melting temperature (T_m) by 8 K (Figure S8 and Table S1). As a result, the T_m for 1A53-2.5 is 32 K higher than T_{opt} . Although 1A53-2.9 is 19 K less stable than 1A53-2.5, its T_m is still 21 K higher than T_{opt} and the kinetic properties of both proteins are very similar. Furthermore, activity loss at high temperature was instantaneous rather than time dependent, inconsistent with temperature-induced unfolding.⁷

Curved Eyring plots can also arise if the activation enthalpy and entropy are temperature dependent.^{7,24,25} Such temperature dependence is manifest as a nonzero activation heat capacity (ΔC_p^\ddagger), which reflects the difference in heat capacity between ground and transition state. Negative ΔC_p^\ddagger values ranging from -0.2 to -3 kcal mol $^{-1}$ K $^{-1}$ have been reported for several enzymes, including ketosteroid isomerase ($\Delta C_p^\ddagger = -0.21$ kcal mol $^{-1}$ K $^{-1}$)⁹ which also catalyzes a proton transfer reaction. Introduction of ΔC_p^\ddagger in the Eyring equation gives eq. 1:⁷

$$\ln(k) = \ln\left(\frac{k_B T}{h}\right) - \frac{[\Delta H_{T_0}^\ddagger + \Delta C_p^\ddagger (T - T_0)]}{RT} + \frac{[\Delta S_{T_0}^\ddagger + \Delta C_p^\ddagger \ln(T/T_0)]}{R} \quad (1)$$

where k_B is the Boltzmann constant, h the Planck constant, and T_0 a reference temperature with corresponding activation enthalpy ($\Delta H_{T_0}^\ddagger$) and entropy ($\Delta S_{T_0}^\ddagger$).⁷ Fitting the temperature data for the evolved eliminases to eq. 1 significantly improved the fits (Figure S7). For 1A53-2.9, the thermodynamic activation parameters at $T_0 = 298$ K were $\Delta H_{T_0}^\ddagger = 5.2 \pm 0.2$ kcal mol $^{-1}$, $\Delta S_{T_0}^\ddagger = -21.0 \pm 0.8$ cal mol $^{-1}$ K $^{-1}$, and $\Delta C_p^\ddagger = -0.29 \pm 0.03$ kcal mol $^{-1}$ K $^{-1}$. Similar parameters were obtained for 1A53-2.5 (Table S1). Comparison with the starting design confirms that the increase in efficiency was achieved entirely by lowering $\Delta H_{T_0}^\ddagger$, offset by an unfavorable activation entropy. In contrast to 1A53-2, the ΔH^\ddagger and $-T\Delta S^\ddagger$ terms for the evolved enzymes contribute nearly equally to the reaction barrier at T_0 . Because the activation parameters are temperature dependent, however, the relative enthalpic and entropic contributions to the barrier are temperature specific (Figure S9). At temperatures below 298 K, the enthalpic term dominates, whereas the entropic term is more important at higher temperatures.

The emergence of an activation heat capacity for this simple chemical reaction is intriguing and may be a thermodynamic signature of the structural changes wrought by molecular evolution of the 1A53-2 scaffold. It has been suggested that curvature in a rate versus temperature plot is a generic property of enzyme-catalyzed reactions, a natural consequence of tight transition state binding affording a more ordered state than the relatively weakly bound enzyme-substrate complex, resulting in a lower relative heat capacity.⁷ Consistent with this view, optimization of 1A53-2 increased the differential stabilization of the transition state ensemble relative to the ground state by more than three orders of magnitude. Thus, the apparent equilibrium constant for dissociation of the transition state from the catalyst [$K_{TS} = k_{uncat}/(k_{cat}/K_M)$] dropped from 63.2 nM to 7.6 pM over the course of evolution, whereas ligand affinity increased roughly twofold assuming $K_M \approx K_s$. The x-ray

data suggest that transformation of the loose binding pocket of the naïve starting catalyst into a tight receptor for the transition state may have been crucial in this regard, reducing the number of conformational states in the transition state ensemble relative to the ground state. Nevertheless, to elucidate the precise physical origins of these effects, further analyses, including molecular dynamics simulations⁹ and calorimetric measurements,^{26,27} will be necessary. Because the binding pocket is buried and hydrophobic, (partially) rate-limiting ligand binding, protein conformational changes, and/or altered active site solvation may also contribute to the observed heat capacity effects.

Our results document the changes in thermodynamic drivers for a computationally designed Kemp eliminase evolved at ambient temperature. As for most natural enzymes, the rate enhancements achieved have enthalpic origins, which became more pronounced as the catalyst evolved. Unexpectedly, the best variants exhibit temperature-dependent activation parameters, which can be explained by the emergence of an activation heat capacity. Similar effects have been observed for some natural biocatalysts⁷ and signal strong adaptation to the conditions of the evolutionary experiments. By adapting our eliminase to higher and lower temperatures, it should be possible to tune T_{opt} and to explore how ΔH^\ddagger and ΔS^\ddagger respond to varying thermal environments.²⁸ Such experiments could shed light on the origins of ΔC_p^\ddagger , as well as its role in the evolution and thermoadaptation of this enzyme and its natural counterparts.

ASSOCIATED CONTENT

Supporting Information

The Supporting Information is available free of charge on the ACS Publications website at DOI: XXX.

Complete experimental procedures and additional kinetic data, including Table S1-S5 and Figures S1-S9 (PDF).

AUTHOR INFORMATION

Corresponding Author

*hilvert@org.chem.ethz.ch

ORCID

H. Adrian Bunzel: 0000-0001-6427-368X
Hajo Kries: 0000-0002-4919-2811
Luca Marchetti: 0000-0002-6100-4465
Cathleen Zeymer: 0000-0001-7138-381X
Peer R. E. Mittl: 0000-0002-3348-3147
Adrian J. Mulholland: 0000-0003-1015-4567
Donald Hilvert: 0000-0002-3941-621X

Author Contributions

H.A.B., H.K. and D.H. designed the experiments. H.A.B., H.K., L.M., and C.Z. performed the experiments. P.M. and H.A.B. recorded the crystallographic data and solved the structure. A.J.M. assisted with the thermodynamic analysis.

Notes

The authors declare no competing financial interests.

ACKNOWLEDGMENTS

The authors thank B. Blattmann and the University Zurich Protein Crystallization Center for help with protein crystallization. This work was supported by the Swiss National Science Foundation and the ETH Zurich. AJM thanks EPSRC (EP/M013219/1 and EP/M022609/1) and BBSRC (BB/M000354/1) for funding.

REFERENCES

- (1) Wolfenden, R., Massive thermal acceleration of the emergence of primordial chemistry, the incidence of spontaneous mutation, and the evolution of enzymes. *J. Biol. Chem.* **2014**, *289*, 30198-30204.
- (2) Wolfenden, R., Benchmark reaction rates, the stability of biological molecules in water, and the evolution of catalytic power in enzymes. *Annu. Rev. Biochem.* **2011**, *80*, 645-667.
- (3) Ciccarelli, F. D.; Doerks, T.; von Mering, C.; Creevey, C. J.; Snel, B.; Bork, P., Toward automatic reconstruction of a highly resolved tree of life. *Science* **2006**, *311*, 1283-1287.
- (4) Knauth, L. P.; Lowe, D. R., High Archean climatic temperature inferred from oxygen isotope geochemistry of cherts in the 3.5 Ga Swaziland Supergroup, South Africa. *Geol. Soc. Am. Bull.* **2003**, *115*, 566-580.
- (5) Gaucher, E. A.; Govindarajan, S.; Ganesh, O. K., Palaeotemperature trend for Precambrian life inferred from resurrected proteins. *Nature* **2008**, *451*, 704-707.
- (6) Akanuma, S.; Nakajima, Y.; Yokobori, S.-i.; Kimura, M.; Nemoto, N.; Mase, T.; Miyazono, K.-i.; Tanokura, M.; Yamagishi, A., Experimental evidence for the thermophilicity of ancestral life. *Proc. Natl. Acad. Sci. U. S. A.* **2013**, *110*, 11067-11072.
- (7) Arcus, V. L.; Prentice, E. J.; Hobbs, J. K.; Mulholland, A. J.; Van der Kamp, M. W.; Pudney, C. R.; Parker, E. J.; Schipper, L. A., On the temperature dependence of enzyme-catalyzed rates. *Biochemistry* **2016**, *55*, 1681-1688.
- (8) Nguyen, V.; Wilson, C.; Hoemberger, M.; Stiller, J. B.; Agafonov, R. V.; Kutter, S.; English, J.; Theobald, D. L.; Kern, D., Evolutionary drivers of thermoadaptation in enzyme catalysis. *Science* **2017**, *355*, 289-294.
- (9) van der Kamp, M. W.; Prentice, E. J.; Kraakman, K. L.; Connolly, M.; Mulholland, A. J.; Arcus, V. L., Dynamical origins of heat capacity changes in enzyme-catalysed reactions. *Nat. Commun.* **2018**, *9*, 1177.
- (10) Kries, H.; Blomberg, R.; Hilvert, D., *De novo* enzymes by computational design. *Curr. Opin. Chem. Biol.* **2013**, *17*, 221-228.
- (11) Kiss, G.; Çelebi-Ölçüm, N.; Moretti, R.; Baker, D.; Houk, K. N., Computational enzyme design. *Angew. Chem. Int. Ed.* **2013**, *52*, 5700-5725.
- (12) Obexer, R.; Godina, A.; Garrabou, X.; Mittl, P. R.; Baker, D.; Griffiths, A. D.; Hilvert, D., Emergence of a catalytic tetrad during evolution of a highly active artificial aldolase. *Nat. Chem.* **2017**, *9*, 50-56.
- (13) Blomberg, R.; Kries, H.; Pinkas, D. M.; Mittl, P. R.; Grütter, M. G.; Privett, H. K.; Mayo, S. L.; Hilvert, D., Precision is essential for efficient catalysis in an evolved Kemp eliminase. *Nature* **2013**, *503*, 418-421.

- (14) Privett, H. K.; Kiss, G.; Lee, T. M.; Blomberg, R.; Chica, R. A.; Thomas, L. M.; Hilvert, D.; Houk, K. N.; Mayo, S. L., Iterative approach to computational enzyme design. *Proc. Natl. Acad. Sci. U. S. A.* **2012**, *109*, 3790-3795.
- (15) Casey, M. L.; Kemp, D. S.; Paul, K. G.; Cox, D. D., Physical organic chemistry of benzisoxazoles. I. Mechanism of the base-catalyzed decomposition of benzisoxazoles. *J. Org. Chem.* **1973**, *38*, 2294-2301.
- (16) Kemp, D. S.; Casey, M. L., Physical organic chemistry of benzisoxazoles. II. Linearity of the Brønsted free energy relation for the base-catalyzed decomposition of benzisoxazoles. *J. Am. Chem. Soc.* **1973**, *95*, 6670-6680.
- (17) Khersonsky, O.; Kiss, G.; Röthlisberger, D.; Dym, O.; Albeck, S.; Houk, K. N.; Baker, D.; Tawfik, D. S., Bridging the gaps in design methodologies by evolutionary optimization of the stability and proficiency of designed Kemp eliminase KE59. *Proc. Natl. Acad. Sci. U. S. A.* **2012**, *109*, 10358-10363.
- (18) Khersonsky, O.; Röthlisberger, D.; Dym, O.; Albeck, S.; Jackson, C. J.; Baker, D.; Tawfik, D. S., Evolutionary optimization of computationally designed enzymes: Kemp eliminases of the KE07 series. *J. Mol. Biol.* **2010**, *396*, 1025-1042.
- (19) Khersonsky, O.; Röthlisberger, D.; Wollacott, A. M.; Murphy, P.; Dym, O.; Albeck, S.; Kiss, G.; Houk, K. N.; Baker, D.; Tawfik, D. S., Optimization of the *in-silico*-designed Kemp eliminase KE70 by computational design and directed evolution. *J. Mol. Biol.* **2011**, *407*, 391-412.
- (20) Dolinsky, T. J.; Nielsen, J. E.; McCammon, J. A.; Baker, N. A., PDB2PQR: an automated pipeline for the setup of Poisson-Boltzmann electrostatics calculations. *Nucleic Acids Res.* **2004**, *32*, W665-W667.
- (21) Genre-Grandpierre, A.; Tellier, C.; Loirat, M.-J.; Blanchard, D.; Hodgson, D. R. W.; Hollfelder, F.; Kirby, A. J., Catalysis of the Kemp elimination by antibodies elicited against a cationic hapten. *Bioorg. Med. Chem. Lett.* **1997**, *7*, 2497-2502.
- (22) Thorn, S. N.; Daniels, R. G.; Auditor, M.-T. M.; Hilvert, D., Large rate accelerations in antibody catalysis by strategic use of haptenic charge. *Nature* **1995**, *373*, 228-230.
- (23) Eyring, H., The activated complex in chemical reactions. *J. Chem. Phys.* **1935**, *3*, 107-115.
- (24) Prabhu, N. V.; Sharp, K. A., Heat capacity in proteins. *Annu Rev Phys Chem* **2005**, *56*, 521-548.
- (25) Oliveberg, M.; Tan, Y. J.; Fersht, A. R., Negative activation enthalpies in the kinetics of protein folding. *Proc. Natl. Acad. Sci. U. S. A.* **1995**, *92*, 8926-8929.
- (26) Firestone, R. S.; Cameron, S. A.; Karp, J. M.; Arcus, V. L.; Schramm, V. L., Heat capacity changes for transition-state analogue binding and catalysis with human 5'-methylthioadenosine phosphorylase. *ACS Chem. Biol.* **2017**, *12*, 464-473.
- (27) Vamvaca, K.; Jelesarov, I.; Hilvert, D., Kinetics and thermodynamics of ligand binding to a molten globular enzyme and its native counterpart. *J. Mol. Biol.* **2008**, *382*, 971-977.
- (28) Åqvist, J.; Kazemi, M.; Isaksen, G. V.; Brandsdal, B. O., Entropy and enzyme catalysis. *Acc Chem Res* **2017**, *50*, 199-207.

Toc Graphic

